Cepharanthine suppresses lung adenocarcinoma through targeting glutathione peroxidase 4

RUOXUE CAO[1-4], SUN KANG[5], KUN WANG[1-4], YAN WANG[3], MINGHUI LI[1-4], QIAN LIU[1-4], YING ZHANG[1-4] and MEI FU[1-4]

[1]Department of Laboratory Medicine, The Second People's Hospital of Lianyungang, Lianyungang, Jiangsu 222006, P.R. China; [2]Department of Clinical Laboratory, Shanghai Municipal Hospital of Traditional Chinese Medicine, Shanghai University of Traditional Chinese Medicine, Shanghai 200071, P.R. China; [3]Department of Laboratory Medicine, Lianyungang Clinical College Xuzhou Medical University and The Second People's Hospital of Lianyungang, Lianyungang, Jiangsu 222006, P.R. China; [4]Department of Laboratory Medicine, Lianyungang Clinical College, Bengbu Medical University and The Second People's Hospital of Lianyungang, Lianyungang, Jiangsu 222006, P.R. China; [5]Department of Hospital Infection Management, The Second People's Hospital of Lianyungang, Lianyungang, Jiangsu 222006, P.R. China

Received September 9, 2025; Accepted April 21, 2026

DOI: 10.3892/ol.2026.15686

Abstract. Lung cancer poses a marked threat to global health, with lung adenocarcinoma (LUAD) being a predominant subtype. Despite their availability, treatment options often fall short of expectations. In this context, Traditional Chinese Medicine, known for its multifaceted therapeutic effects and favorable safety profile, has emerged as a promising alternative. In particular, cepharanthine (CEP), a bisbenzylisoquinoline alkaloid derived from *Stephania cepharantha*, has demonstrated the ability to suppress the proliferation of a range of tumor cells. However, the precise mechanisms by which CEP impacts LUAD remain to be elucidated. The present study focused on the anti-tumor effects of CEP on LUAD. Cellular experiment analysis revealed that CEP exhibited an IC_{50} value of 6.810 μM for the H1299 cell line and 9.041 μM for the PC-9 cell line, with minimal toxicity to normal BEAS-2B cells. Bioinformatics analysis identified three potential target genes for CEP, namely glutathione peroxidase 4 (GPX4), tyrosyl-DNA phosphodiesterase 1 and carbonic anhydrase 4, among which CEP significantly suppressed the expression of GPX4 in LUAD cells. Further validation showed that the impact of CEP on cell proliferation, apoptosis and invasiveness was diminished in cells with GPX4 knockdown. *In vivo* experiments demonstrated that CEP could inhibit the growth of subcutaneously transplanted tumors in mice, however its therapeutic effect was reduced in GPX4 gene knockout mice bearing GPX4-knockdown tumors. In summary, CEP may exert its anti-LUAD effects by targeting GPX4, thereby offering a novel therapeutic strategy for LUAD treatment.

Correspondence to: Dr Mei Fu, Department of Laboratory Medicine, The Second People's Hospital of Lianyungang, 41 East Hailian Road, Lianyungang, Jiangsu 222006, P.R. China
E-mail: fumei.1234@163.com

Key words: lung adenocarcinoma, cepharanthine, Gene Expression Omnibus, glutathione peroxidase 4

Introduction

Lung cancer, a prevalent malignant neoplasm of the respiratory system, poses a marked threat to global health (1). It is characterized by chronic coughing, hemoptysis and pulmonary opacities. The primary risk factors associated with lung cancer include smoking, exposure to radon, asbestos, air pollution and a familial predisposition to the disease (2). Lung cancer stands as the primary cause of cancer-associated mortality in men and the second in women. In 2018, it claimed the lives of 1.2 million men and 576,100 women, representing 18.4% of all cancer mortalities (3). By 2020, lung cancer had accounted for 2.2 million new cases worldwide, which was 11.4% of all new cancer diagnoses, with 1.796 million (18%) total global cancer mortalities (4). The continued rise in lung cancer mortality rates in China in previous years is a concerning trend that warrants attention (5).

Lung adenocarcinoma (LUAD), the most prevalent subtype of non-small cell lung cancer, constitutes ~40% of all lung malignancies. Treatment strategies are tailored according to disease stage, with surgical resection being the primary treatment for early-stage patients who are suitable surgical candidates (6,7). However, the initial presentation of LUAD is often discreet and due to the constraints in screening and diagnostic methods, the majority of patients are diagnosed at later stages when surgical intervention may no longer be an option. For these patients, chemotherapy and radiation therapy have become the primary treatment options (8). In previous years, marked progress has been made in targeted therapy and immunotherapy, offering promising treatment options for LUAD patients with specific genetic mutations, including EGFR, ALK receptor tyrosine kinase, ROS proto-oncogene 1 and BRAF (9,10). Despite their potential, targeted therapies

are often expensive and may not be beneficial for numerous Chinese patients who lack the necessary receptors for these drugs, thus limiting their accessibility. Furthermore, immunotherapy may be associated with side effects such as dermatitis and drug resistance and in some cases, it may even accelerate tumor progression, making it an unsuitable option for all patients (11). Consequently, chemotherapy remains a mainstay for advanced lung cancer treatment. The standard first-line chemotherapy for LUAD typically involves a combination of platinum-based drugs with agents such as gemcitabine, paclitaxel, vinorelbine or docetaxel (12-15). However, research indicates that the overall response rate to first-line chemotherapy is suboptimal and the side effects can severely impact the quality of life for patients, leading a number of individuals to decline second-line chemotherapy after an initial failure (16).

Traditional Chinese Medicine (TCM), a key component of Chinese medical heritage, is known for its multifaceted, multitargeted and multipotent approach with a favorable safety profile (17). A notable body of research has indicated that TCM holds marked advantages in the treatment of LUAD. Its gentle efficacy and high safety profile not only mitigate the side effects of radiotherapy and chemotherapy but also greatly benefit patient lifespan and the improve their quality of life, as well as their median survival period (18-21). Amongst the escalating incidence of cancer and increasing resistance to chemotherapeutic drugs, there is an urgent need to further explore and harness the potential of TCM. Elucidating its mechanisms of action against cancer is key in developing safer, more effective and cost-efficient treatment options for patients with advanced LUAD.

Stephania cepharantha, a traditional Chinese medicinal herb from the *Menispermaceae* family, has been widely valued for its diverse applications in medicine (22-24). For example, Chen *et al* (25) found that cepharanthine induces oxidative stress and apoptosis in cervical cancer cells via the Nrf2/Keap1 pathway. Contemporary clinical and pharmacological studies have demonstrated its multifaceted pharmacological properties, such as hemostasis, fever reduction, antibacterial and anti-inflammatory effects, analgesic actions, detoxification, diuretic effects and anti-edematous capabilities (26,27). Cepharanthine (CEP), a bisbenzylisoquinoline alkaloid derived from *Stephania cepharantha* and *Tripterygium wilfordii*, has previously shown to exhibit a range of bioactivities (28). These include anti-tumor, anti-aging, leukocytosis-inducing, antiviral, immune-modulatory, antimalarial and anti-inflammatory effects, as well as the prevention of lipopolysaccharide-induced lung vascular damage (29-32). Notably, the anti-tumor activity of CEP has been particularly well-documented, with its mechanisms of action encompassing the inhibition of cancer cell proliferation, the induction of cancer cell redifferentiation, the initiation of apoptosis, the reversal of multidrug resistance in tumors, the enhancement of chemotherapeutic drug efficacy and the suppression of tumor infiltration and metastasis (33-35). However, the role and underlying mechanisms of CEP in LUAD remain unexplored.

Therefore, the present study aimed to explore the anti-tumor effects of CEP through cellular and animal experiments, complemented by bioinformatics analysis to provide initial insights into its mechanisms of action.

Materials and methods

Cell culture and experimental grouping. Human LUAD cell lines H1299 and PC-9, obtained from the Cell Resource Center at the Shanghai Institutes for Biological Sciences, Chinese Academy of Sciences (Shanghai, China) and human lung bronchial epithelial cells BEAS-2B, procured from Wuhan Pricella Biotechnology Co., Ltd., were cultivated in DMEM medium supplemented with 10% FBS and 1% penicillin-streptomycin antibiotic mixture. All the cells were maintained in a humidified incubator at 37˚C with 5% CO_2. To initiate the experiment, cells were exposed to a range of CEP concentrations (0-64 μM; purity >98%; cat. no. 481-49-2; Shanghai Yuanye Bio-Technology Co., Ltd.) for a period of 24 h in a humidified incubator at 37˚C with 5% CO_2. Subsequently, cell viability was assessed using a Cell Counting Kit-8 (CCK-8) assay to determine the IC_{50} values. For the experiments, H1299 and PC-9 cells were randomly assigned to three groups: Control, CEP-L (low dose) and CEP-H (high dose). The Control group was untreated, whereas the CEP-H group was treated with a CEP concentration equivalent to the IC_{50} value determined for LUAD cells. The CEP-L group was treated with a CEP concentration at 50% of the IC_{50} value.

Genetic knockdown (KD). To mitigate the potential for off-target effects, three distinct short hairpin (sh)-RNAs were designed specifically targeting glutathione peroxidase 4 (GPX4) in the present study. The sequences were as follows: GPX4 shRNA#1, 5'-GTGAGGCAAGACCGAAGTAAA-3'; GPX4 shRNA#2, 5'-GGGAGTAACGAAGAGATCAAA-3'; GPX4 shRNA#3, 5'-GACCGAAGTAAACTACACTCA-3'; and shRNA-negative control (NC), 5'-TTCTCCGAACGTGTC ACGT-3'. H1299 and PC-9 cells were diluted with DMEM medium to form a uniform layer and once they reached ~70% confluence, the medium was carefully replaced with serum-free DMEM containing 1% penicillin-streptomycin (cat. no. 15140122; Gibco; Thermo Fisher Scientific, Inc.). For each well of a 6-well plate, 2.5 μg of shRNA plasmid was diluted in 125 μl Opti-MEM reduced serum medium (cat. no. 31985070; Gibco; Thermo Fisher Scientific, Inc.), and 6.25 μl Lipofectamine® 3000 reagent (cat. no. L3000150; Invitrogen; Thermo Fisher Scientific, Inc.) was separately diluted in 125 μl Opti-MEM. After 5 min of incubation at room temperature (RT), the two solutions were combined, gently mixed and incubated for an additional 10-15 min at RT to allow transfection complex formation. The shRNAs were transfected into the cells using Lipofectamine® 3000 reagent according to the manufacturer's protocol. Following transfection, all cells were incubated in a cell culture incubator at 37˚C with 5% CO_2. After incubation, the cells were collected for further experimental procedures.

CCK-8 assay. Cells exposed to different concentrations of CEP were plated into a 96-well plate at a density of $3x10^3$ cells per well, with each group having five replicate wells. The plate was then incubated in a cell culture incubator at 37˚C with 5% CO_2 for 24 h. Subsequently, 10 μl CCK-8 reagent (MilliporeSigma; Merck KGaA) was added to each well. After incubating for an additional 1 h under the same conditions, the optical density (OD) at 450 nm was measured using a microplate reader

(Bio-Rad Laboratories, Inc.). The OD values of the control group were normalized to 100% and the IC_{50} curves for the CEP treatments were graphed accordingly.

Clone formation assay. Cells exhibiting robust proliferation from each group were plated into 12-well plates at a density of $1x10^3$ cells per well, with each group having three replicate wells. They were cultured in a humidified incubator at 37˚C with 5% CO_2 and the medium was refreshed every 3-4 days. Colony formation was observed as the development of macroscopic cell colonies (defined as clusters of ≥50 cells) ~2 weeks post-seeding. Thereafter, the cells were fixed with 4% paraformaldehyde for 30 min at RT, followed by staining with 0.1% crystal violet for 15 min at RT. Nonspecific materials, including excess dye, were washed away with PBS buffer until dry. Finally, images were captured and colonies were enumerated manually under a light microscope to assess cloning efficiency.

TUNEL staining assay. Adhering to the protocol outlined in the TUNEL Apoptosis Detection Kit (Abcam), the detailed procedure was as follows: Initially, the treated cells were rinsed with PBS twice, fixed with 4% paraformaldehyde for 30 min at RT and then rinsed with PBS for 5 min (a total of three times). Next, 20% normal bovine serum was added and the cells were incubated at RT for 30 min to block non-specific binding. Afterwards, the TUNEL reaction mixture was applied to the sections and incubated at 37˚C for 90 min (for negative controls, the terminal deoxynucleotidyl transferase enzyme was excluded from the TUNEL mixture). Next, the cells were rinsed with PBS for 5 min (a total of three times), before DAPI was added for nuclear counterstaining and further incubation was carried out in the dark at RT for 10 min. Following an additional rinse with PBS for 5 min (a total of three times), the sections were mounted with an anti-fade mounting medium and examined under a fluorescence microscope. For each sample, at least five random fields of view were captured and analyzed.

Transwell assay. H1299 and PC-9 cells from each group in the logarithmic growth phase were serum-starved for 24 h. The Transwell chamber inserts were pre-coated with Matrigel and incubated for at least 4 h at 37˚C to allow polymerization. Subsequently, 0.2 ml cell suspension was added to the upper compartment of the Matrigel-coated Transwell chamber, while 700 μl pre-warmed DMEM supplemented with 10% FBS was placed in the lower compartment. The chamber was then incubated at 37˚C in a cell culture incubator with 5% CO_2 for 24 h. Afterward, cells on the upper surface of the membrane and the basal side were gently removed with a wet cotton swab. The cells were fixed with methanol for 30 min at RT and stained with 0.1% crystal violet for 20 min at RT. Finally, the cells were examined and photographed using an inverted light microscope (Olympus Corporation). Randomly selected fields of view were used to quantify the number of cells that had migrated across the membrane.

Western blotting. Cells were collected and rinsed three times with PBS, followed by lysis using RIPA buffer supplemented with protease and phosphatase inhibitors (Cell Signaling Technology, Inc.) for 10 min on ice. Protein concentrations were measured using a Bio-Rad protein assay. Equivalent amounts of protein samples (20 μg per lane) were resolved by 12% SDS-PAGE and transferred onto PVDF membranes (MilliporeSigma; Merck KGaA). Membranes were then blocked with 5% skim milk for 1 h at RT. Primary antibodies were applied and incubated overnight at 4˚C, followed by incubation with HRP-conjugated secondary antibodies (1:3,000; Santa Cruz Biotechnology, Inc.) for 1 h at RT. Specific details for each antibody, including dilution and manufacturer, are provided in Table SI. After ECL detection using the Pierce ECL Western Blotting Substrate (Thermo Fisher Scientific, Inc.), grayscale analysis was conducted using ImageJ software (version 1.53t; National Institutes of Health) and densitometric analysis was performed using Image-Pro Plus (version 6.0; Media Cybernetics, Inc.) software. The relative protein expression levels in each group were normalized to β-actin as an internal control, with the target protein content of the control group set to a value of 1. Each experiment was conducted in triplicate.

Quantitative real-time polymerase chain reaction (RT-qPCR). Total cellular RNA was extracted using TRIzol reagent (Invitrogen; Thermo Fisher Scientific, Inc.), followed by reverse transcription into cDNA in accordance with the protocols provided by the reverse transcription kit (GoScript™ Reverse Transcription System; Promega Corporation). Subsequently, qPCR was conducted using SYBR® Green I (Thermo Fisher Scientific, Inc.) as the fluorophore. The thermocycling conditions were as follows: Initial denaturation at 95˚C for 10 min, followed by 40 cycles of denaturation at 95˚C for 15 sec, annealing at 60˚C for 30 sec and extension at 72˚C for 30 sec. β-actin served as an endogenous control and the relative mRNA expression levels of GPX4, tyrosyl-DNA phosphodiesterase 1 (TDP1) and carbonic anhydrase 4 (CA4) were determined using the $2^{-\Delta\Delta Cq}$ method (36). The sequences of RT-qPCR primers used are outlined in Table SII.

Bioinformatics analysis. Microarray datasets pertinent to LUAD were sourced from the Gene Expression Omnibus (GEO) database, a comprehensive public gene expression repository established by the National Center for Biotechnology Information in the United States (https://www.ncbi.nlm.nih.gov/geo/). Specifically, the GSE10799 dataset (37) from the GPL570 platform ('HG-U133_Plus_2 Affymetrix Human Genome U133 Plus 2.0 Array') was accessed, encompassing 16 LUAD samples and 3 normal samples. In addition, the GSE31547 dataset (38) from the GPL96 platform ('HG-U133A Affymetrix Human Genome U133A Array') was utilized, which includes 30 LUAD samples and 20 normal samples. These datasets underwent background correction and normalization preprocessing using the 'Limma' R software package (39) prior to analysis. The threshold for identifying differentially expressed genes (DEGs) was set at log (fold change) ≥0.5 with an adjusted P-value <0.05. Subsequently, potential target genes of CEP were investigated using both the Search Tool for Interactions of Chemicals (STITCH; https://ngdc.cncb.ac.cn/databasecommons/database/) and TCM Systems Pharmacology Database and Analysis Platform (TCMSP; https://old.tcmsp-e.com/tcmsp.php) databases.

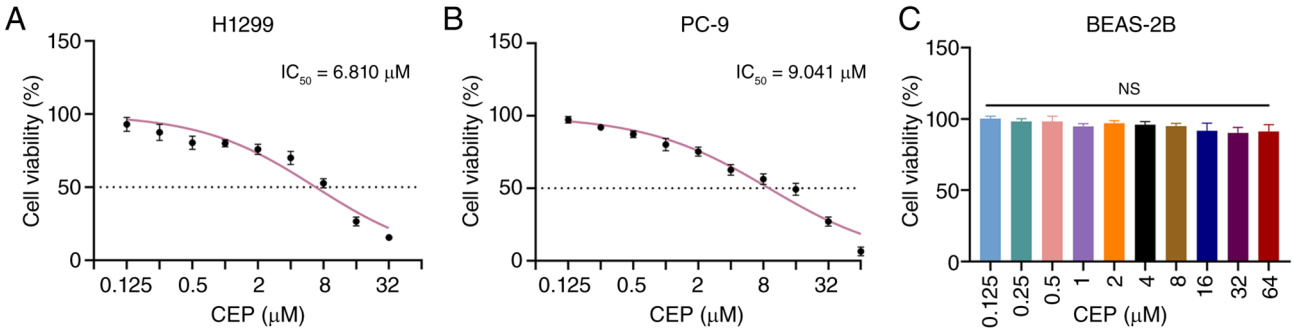

Figure 1. Impact of CEP on the viability of lung adenocarcinoma cells and human lung bronchial epithelial cells. (A) H1299 cells were exposed to a series of CEP concentrations for 24 h, after which cell viability was evaluated using a CCK-8 assay and the IC_{50} value was determined. (B) PC-9 cells were subjected to a range of CEP concentrations for 24 h, followed by assessment of cell viability using a CCK-8 assay and calculation of the IC_{50} value. (C) Human lung bronchial epithelial cells BEAS-2B were treated with varying concentrations of CEP for a period of 24 h and cell viability was subsequently measured using a CCK-8 assay. Data are presented as the mean ± SEM (n=3). CEP, cepharanthine; NS, not significant (P>0.05); CCK-8, Cell Counting Kit-8.

Mouse xenograft tumor model experiment. To investigate dependency of the anti-tumor efficacy of CEP on GPX4, both wild-type (WT) and GPX4 knockout (KO) mice (C57BL/6JCya-Gpx4em1flox/Cya; Cyagen) were utilized to establish a dual-targeting validation model. All animal procedures were performed in strict accordance with the National Institutes of Health Guide for the Care and Use of Laboratory Animals (40) and were approved by the Animal Care and Use Committee of the Second People's Hospital of Lianyungang (approval no. 2023K022). A total of 25 C57BL/6J male mice (5-6 weeks old, weighing 18-22 g) were used in the present study. WT mice were randomly divided into three groups (n=5 per group): A control group receiving PBS and two treatment groups receiving CEP at doses of 5 and 10 mg/kg, respectively. LUAD xenograft tumor models in WT mice were established by subcutaneously injecting 0.5 ml WT H1299 cells into the right inguinal region. Conversely, to create a 'comprehensive GPX4-null' environment and rule out the influence of host microenvironmental GPX4, the remaining 10 GPX4 KO mice were injected with H1299 cells that had been pre-transfected with GPX4 shRNA#3 (GPX4-KD cells). These mice served as a stringent NC to validate the absolute requirement of the GPX4 target for the mechanism of action of CEP.

The specific humane endpoints for euthanasia were predefined as: i) Tumor volume exceeding 1,500 mm^3; ii) notable body weight loss (>20% of initial body weight); or iii) signs of severe distress such as lethargy, inability to access food or water or labored breathing. Throughout the entire 42-day experimental period, no animals reached these humane endpoints or were found to be deceased spontaneously; all 25 animals that entered the present study were accounted for at its conclusion. Animal health and behavior were monitored twice daily (morning and evening) by trained personnel for any signs of pain, distress or adverse effects. To minimize suffering, all surgical procedures for tumor cell implantation were performed under anesthesia induced by intraperitoneal injection of a mixture of 100 mg/kg ketamine and 10 mg/kg xylazine. The injection site was disinfected with 75% ethanol prior to the subcutaneous injection of tumor cells. Post-operatively, mice were placed on a heating pad until fully recovered from anesthesia. All mice were housed in a specific pathogen-free facility under controlled conditions (temperature: 22±2˚C; humidity: 50±10%; 12-h light/dark cycle) with free access to sterile food and water. The tumor model was determined when the tumor reached a size of 0.4x0.4 cm^2, along with signs such as weight loss, mobility impairment and dry fur.

The experimental groups were administered CEP through intraperitoneal injection at the specified doses once daily for a period of 42 days. The control group received an equivalent volume of physiological saline through intraperitoneal injection once daily for the same duration. At the end of the 42-day treatment period, all mice were euthanized by cervical dislocation following deep anesthesia with the aforementioned ketamine/xylazine mixture. Mortality was verified by the absence of both respiratory movement and heartbeat, further verified by palpation. Subsequently, the tumors were harvested and weighed.

Statistical analysis. Data in the present study are presented as mean ± SEM. In all experiments, n represents the number of independent biological replicates. Statistical analysis was conducted using GraphPad Prism (version 8.0.; Dotmatics). The Student's t-test was employed to assess significant differences between two groups, while one-way ANOVA was utilized to compare differences across multiple groups. P<0.05 was considered to indicate a statistically significant difference.

Results

Impact of CEP on the viability of LUAD cells and human lung bronchial epithelial cells. Initially, a range of CEP concentrations were applied to H1299 and PC-9 cell lines for a duration of 24 h to determine the IC_{50} values for these cells. The findings revealed that the IC_{50} for H1299 cells was 6.810 μM (Fig. 1A), while for PC-9 cells it was 9.041 μM (Fig. 1B). Based on these values, the high dose group was assigned the CEP concentration equivalent to the IC_{50} and the low dose group was given half of that concentration for subsequent experiments. Furthermore, to evaluate the safety profile of CEP on normal cells, the impact of varying CEP concentrations on the vitality of human lung bronchial epithelial cells BEAS-2B was also assessed. As shown in Fig. 1C, no significant alteration in cell viability was observed post-CEP treatment, suggesting that CEP

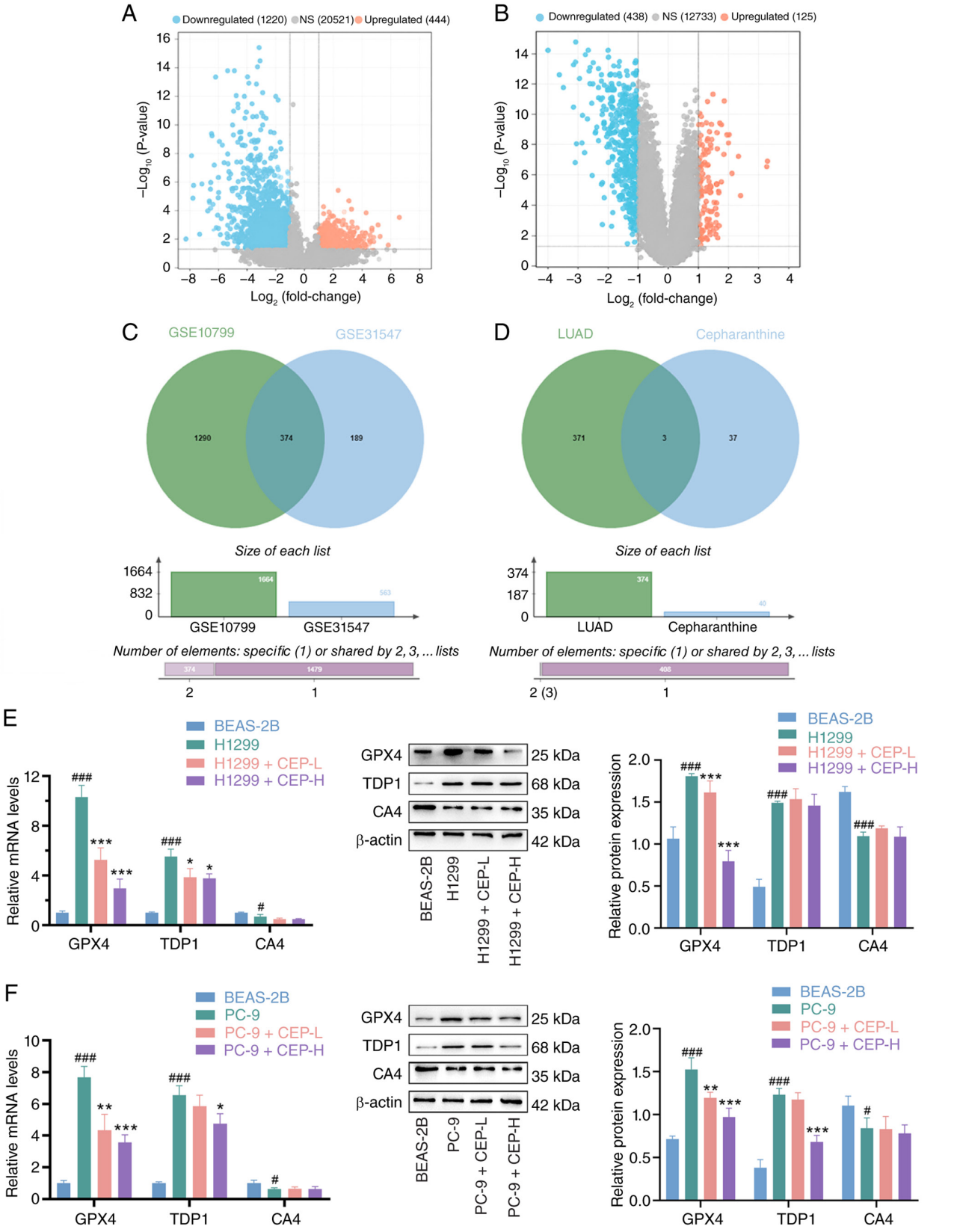

Figure 2. Bioinformatics-driven identification of potential CEP targets in LUAD. (A) Volcano plot illustrating the DEGs from the GSE10799 dataset, consisting of 16 LUAD samples and 3 normal samples. (B) Volcano plot representing the DEGs from the GSE31547 dataset, comprising 30 LUAD samples and 20 normal samples. (C) Venn diagram displaying the intersection of DEGs identified in the GSE10799 and GSE31547 datasets. (D) Venn diagram showing the intersection of potential CEP target genes from the Search Tool for Interactions of Chemicals and Traditional Chinese Medicine Systems Pharmacology Database and Analysis Platform databases with the 374 DEGs associated with LUAD. (E) RT-qPCR and western blotting analysis were conducted to measure the mRNA and protein expression levels of GPX4, TDP1 and CA4 in BEAS-2B cells and H1299 cells treated with varying concentrations of CEP. (F) RT-qPCR and western blotting analysis were utilized to evaluate the mRNA and protein expression levels of GPX4, TDP1 and CA4 in BEAS-2B cells and PC-9 cells exposed to high and low doses of CEP. Data are presented as the mean ± SEM (n=3). *P<0.05, **P<0.01 and ***P<0.001; $^{\#}$P<0.05 and $^{\#\#\#}$P<0.001. CEP, cepharanthine; LUAD, lung adenocarcinoma; CEP-L, CEP-low; CEP-H, CEP-high; NS, not significant; GPX4, glutathione peroxidase 4; TDP1, tyrosyl-DNA phosphodiesterase 1; CA4, carbonic anhydrase 4; DEGs, differentially expressed genes; RT-qPCR, reverse transcription quantitative PCR.

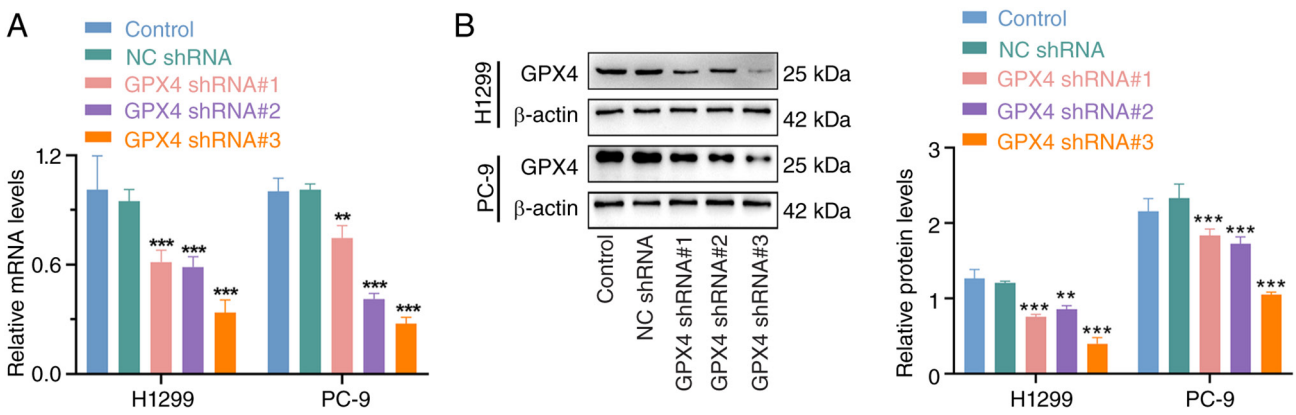

Figure 3. Verification of GPX4 knockdown efficiency in lung adenocarcinoma cells. (A) RT-qPCR was utilized to assess the mRNA expression levels of GPX4 in H1299 and PC-9 cells following transfection with GPX4 shRNA#1, GPX4 shRNA#2 and GPX4 shRNA#3. (B) Western blotting analyses was employed to evaluate the protein expression levels of GPX4 in H1299 and PC-9 cells after transfection with GPX4 shRNA#1, GPX4 shRNA#2 and GPX4 shRNA#3. Data are presented as the mean ± SEM (n=3). **P<0.01 and ***P<0.001. GPX4, glutathione peroxidase 4; NC, negative control; shRNA; short hairpin RNA; NS, not significant.

exhibited minimal toxicity towards normal cells and thus has a favorable safety profile.

Bioinformatics-driven identification of potential CEP targets in LUAD. In the present study, two GEO datasets (GSE10799 and GSE31547) were encompassed, each comprising LUAD and normal tissue samples. Differential expression analysis revealed 1,664 DEGs in the GSE10799 dataset, with 444 being upregulated and 1,220 downregulated (Fig. 2A). The GSE31547 dataset uncovered 563 DEGs, including 125 upregulated and 438 downregulated genes (Fig. 2B). By intersecting the DEGs from both datasets, a core set of 374 overlapping DEGs was identified, such as SPTBN1, ADGRB3, FHL1, GDF10, FAM107A, GRIA1, ASPA, ITGA8, CALCRL, SGCG, PTPRB and others (Fig. 2C).

Subsequently, STITCH and TCMSP databases were used to predict potential CEP target genes, identifying a total of 40 candidates. The intersection with the 374 LUAD DEGs yielded three genes: GPX4, TDP1 and CA4 (Fig. 2D). To validate the expression of these hub genes, RT-qPCR and western blotting was employed to assess their levels in BEAS-2B, H1299 and PC-9 cells, as well as in LUAD cells treated with high and low doses of CEP. As shown in Fig. 2E and F, GPX4 and TDP1 were significantly upregulated in the LUAD cell line H1299 compared with BEAS-2B cells, while CA4 was significantly downregulated. In addition, CEP treatment led to a dose-dependent decrease in GPX4 expression, a milder reduction in TDP1 and no significant change in CA4 expression. These findings indicate that CEP markedly suppressed GPX4 expression in LUAD cells, suggesting its potential as a therapeutic target.

Verification of GPX4 KD efficiency in LUAD cells. In order to further explore the role of GPX4 as a potential therapeutic target of CEP in the malignancy of LUAD, the present study constructed three distinct shRNAs targeting GPX4 to mitigate the possibility of off-target effects. Upon transfection of these shRNAs into H1299 and PC-9 cells, both RT-qPCR and western blotting analyses demonstrated that GPX4 shRNA#1, GPX4 shRNA#2 and GPX4 shRNA#3 significantly decreased the expression of GPX4 at both the mRNA (Fig. 3A) and protein levels (Fig. 3B). Notably, GPX4 shRNA#3 exhibited the most efficient silencing efficacy. Therefore, it was selected for further experimental investigation.

KD of GPX4 renders CEP ineffective on LUAD cell behavior. Subsequently, H1299 and PC-9 cells transfected with either NC shRNA or GPX4 shRNA#3 were subjected to treatment with high and low doses of CEP. Fig. 4 illustrates that in cells transfected with NC shRNA, CEP intervention significantly dose-dependently suppressed cell proliferation (Fig. 4A), significantly induced apoptosis (Fig. 4B) and significantly inhibited cell invasion (Fig. 4C). By contrast, Fig. 5 demonstrates that in H1299 and PC-9 cells transfected with GPX4 shRNA#3, CEP treatment at both concentrations failed to significantly impact cell proliferation (Fig. 5A), apoptosis (Fig. 5B) or invasion capabilities (Fig. 5C). This observation suggests that the KD of GPX4 may have resulted CEP therapeutic target loss, thereby rendering it ineffective.

CEP inhibits the growth of subcutaneous xenografted tumors in mice by suppressing GPX4. Within the present study, the effects of CEP on LUAD cells *in vitro* were examined and thus, the investigation was extended to explore the *in vivo* impact of CEP on tumor growth in C57BL/6J mice with xenografted tumors. First, LUAD mouse xenograft models were established by inoculating H1299 cells into WT mice, followed by treatment with CEP at doses of 5 and 10 mg/kg through intraperitoneal injection. The findings revealed a significant reduction in the size of xenografted tumors post-CEP treatment, with the 10 mg/kg dose exhibiting the most significant effect. In addition, tumor volume and weight were significantly decreased in a dose-dependent manner in response to CEP treatment (Fig. 6A).

To further validate the dependency of the anti-tumor activity of CEP on GPX4, a 'comprehensive GPX4-null' model was established. This was achieved by utilizing GPX4 gene-KO mice (C57BL/6JCya-Gpx4em1flox/Cya) and inoculating them with H1299 cells that had been stably transfected with GPX4 shRNA#3, thereby ablating GPX4 expression in

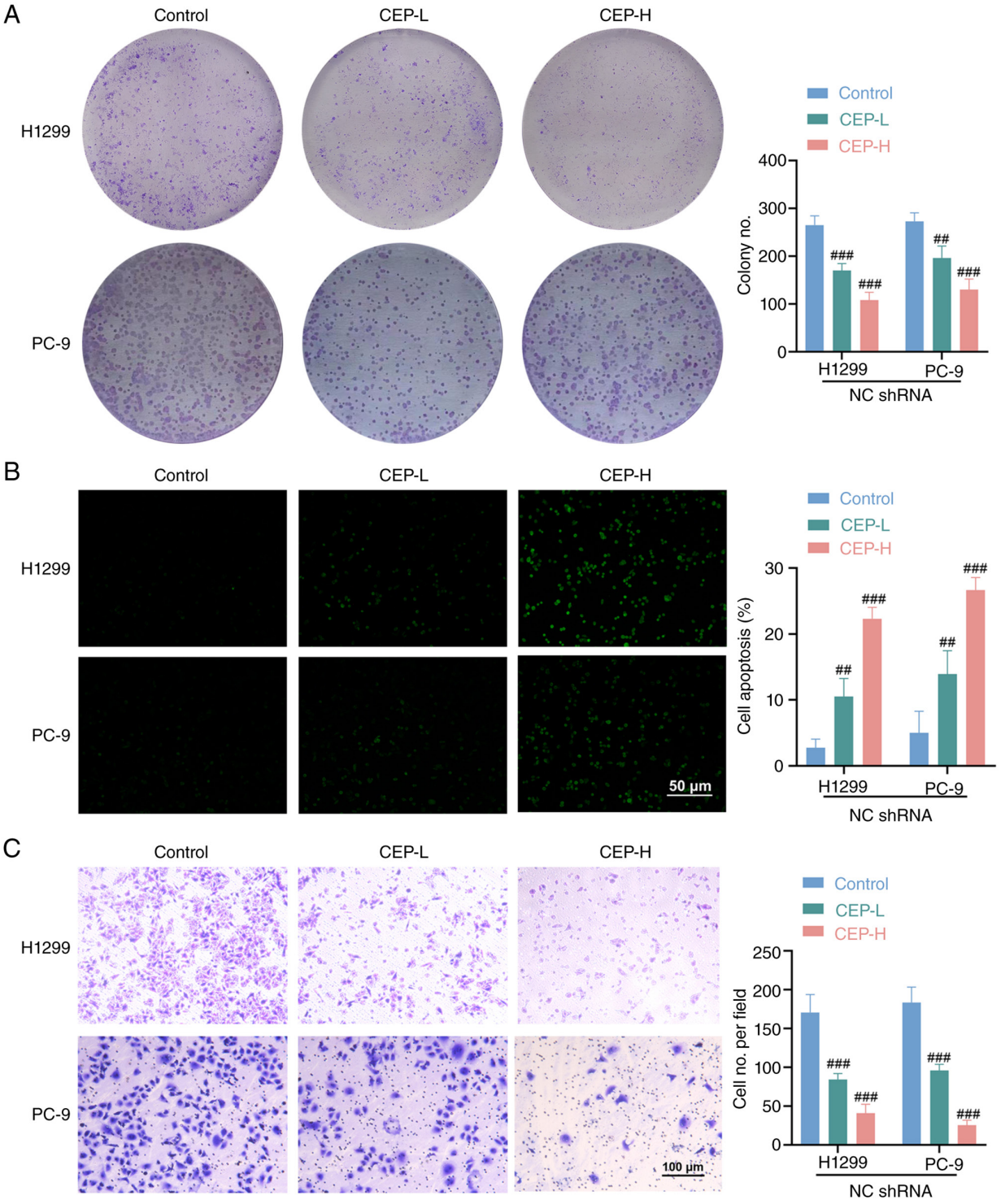

Figure 4. Inhibitory effects of CEP on lung adenocarcinoma cell proliferation and invasion and induction of apoptosis. (A) A clone formation assay was conducted to evaluate the impact of CEP treatment at low and high doses on the proliferation of H1299 and PC-9 cells transfected with NC shRNA. (B) A TUNEL assay was conducted to determine the impact of CEP treatment at low and high doses on apoptosis in H1299 and PC-9 cells transfected with NC shRNA. (C) A Transwell invasion assay was employed to assess the impact of CEP treatment at low and high doses on the invasive capabilities of H1299 and PC-9 cells transfected with NC shRNA. Data are presented as the mean ± SEM (n=3). $^{##}$P<0.01 and $^{###}$P<0.001. CEP, cepharanthine; CEP-L, CEP-low; CEP-H, CEP-high; NC, negative control; shRNA; short hairpin RNA.

both the host microenvironment and the tumor cells. These mice were then treated with CEP at doses of 5 and 10 mg/kg through intraperitoneal injection. The results demonstrated that in this 'comprehensive GPX4-null' system, the antitumor effect of CEP was significantly attenuated compared to its effect in WT mice, but not completely abolished. As shown in Fig. 6B, tumor weight and volume in both the CEP (5 mg/kg) and CEP (10 mg/kg) treatment groups were still significantly lower than those in the PBS control group (P<0.05). However, the magnitude of this reduction was markedly smaller than that observed in the WT mouse model (Fig. 6A). These *in vivo* experiments further validated the cellular experimental

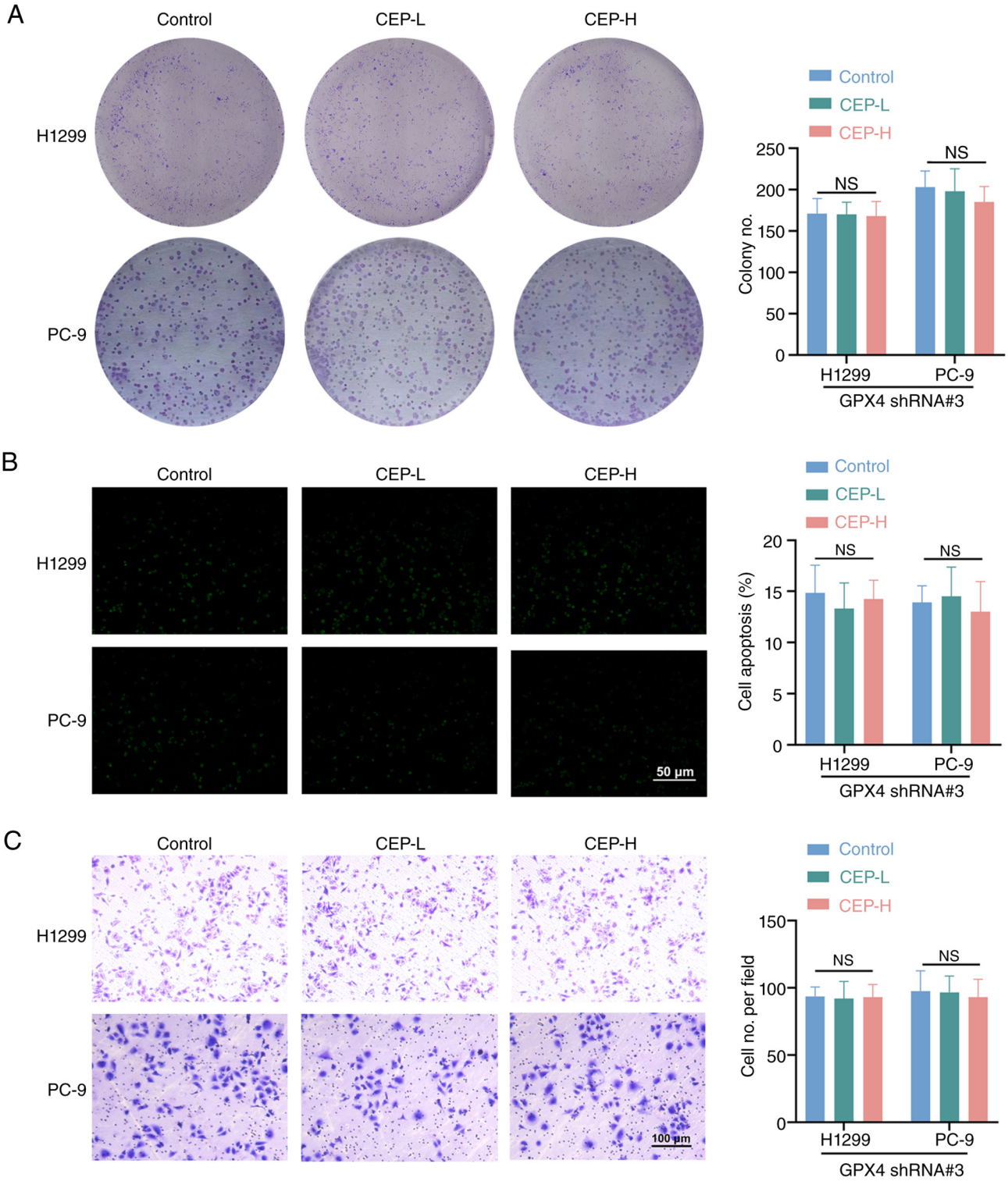

Figure 5. Knockdown of GPX4 renders CEP ineffective on lung adenocarcinoma cell behavior. (A) A clone formation assay was conducted to evaluate the impact of CEP treatment at low and high doses on the proliferation of H1299 and PC-9 cells transfected with GPX4 shRNA#3. (B) A TUNEL assay was conducted to determine the impact of CEP treatment at low and high doses on apoptosis in H1299 and PC-9 cells transfected with GPX4 shRNA#3. (C) A Transwell invasion assay was employed to assess the impact of CEP treatment at low and high doses on the invasive capabilities of H1299 and PC-9 cells transfected with GPX4 shRNA#3. Data are presented as the mean ± SEM (n=3). CEP, cepharanthine; CEP-L, CEP-low; CEP-H, CEP-high; shRNA, short hairpin RNA, GPX4, glutathione peroxidase 4; NS, not significant (P>0.05).

outcomes. In conclusion, CEP effectively suppresses the proliferation of LUAD cells and xenografted tumors in mice, but the therapeutic benefits of CEP are substantially diminished when GPX4 is knocked down in both the tumor and the host microenvironment.

Discussion

Lung cancer is a marked threat to global health, with LUAD representing a predominant subtype (41). While there have been improvements in detection and therapeutic strategies, numerous

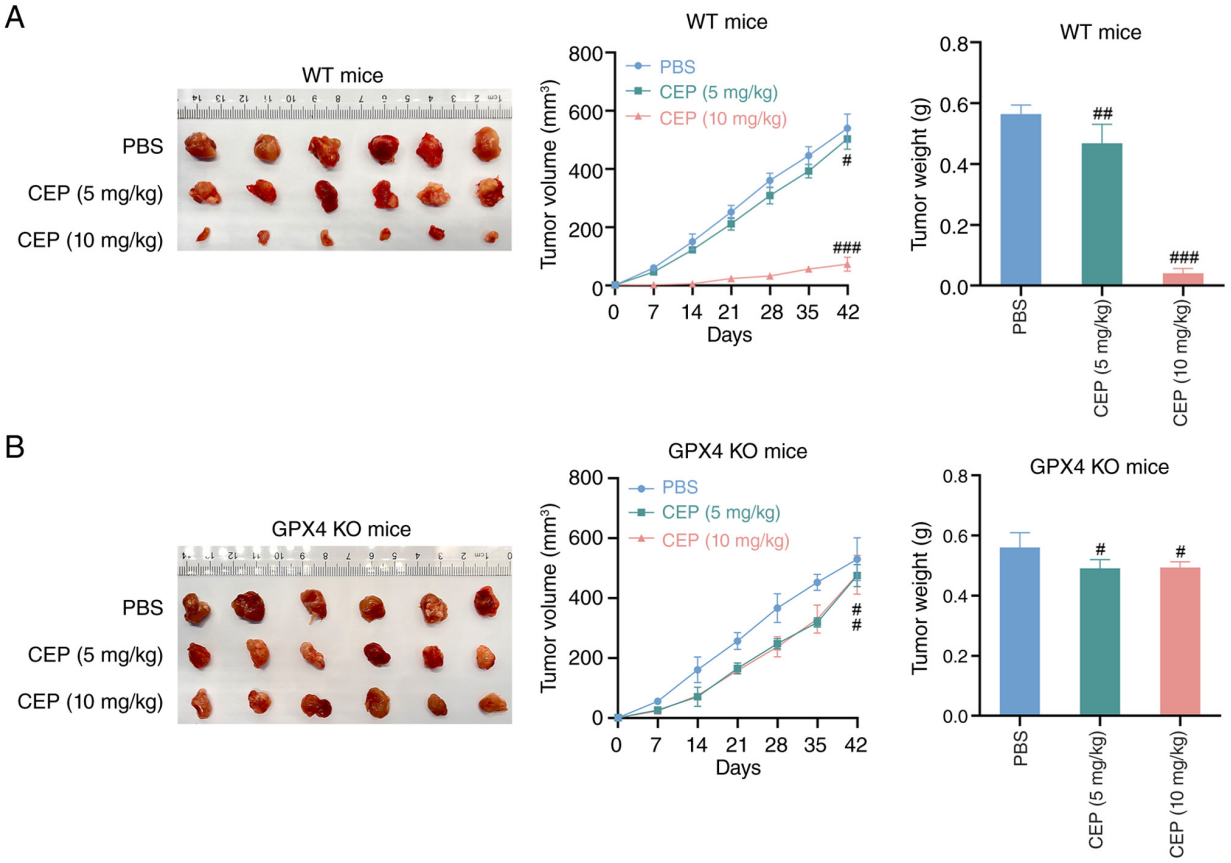

Figure 6. CEP inhibits the growth of subcutaneous xenografted tumors in mice by suppressing GPX4. (A) H1299 cells were injected into WT mice to establish a LUAD mouse xenograft model, followed by treatment with CEP at doses of 5 and 10 mg/kg through intraperitoneal injection. After 42 days, the mice were euthanized and tumor volume and weight were measured. (B) GPX4 gene-KO mice were generated by injecting H1299 cells transfected with GPX4 shRNA#3 to establish a LUAD mouse xenograft model, followed by treatment with CEP at doses of 5 and 10 mg/kg through intraperitoneal injection. After 42 days, the mice were euthanized and tumor volume and weight were measured. Data are presented as the mean ± SEM (n=5). $^{\#}$P<0.05, $^{\#\#}$P<0.01 and $^{\#\#\#}$P<0.001. CEP, cepharanthine; GPX4, glutathione peroxidase 4; WT, wild-type; KO, knockout; LUAD, lung adenocarcinoma; shRNA, short hairpin RNA.

patients with LUAD are still diagnosed at late stages, leaving chemotherapy and radiation as the main treatment avenues. Although targeted therapies and immunotherapies have demonstrated potential (42), their high costs and side effect profiles may preclude their use in some patients. In this context, TCM, known for its holistic approach and favorable safety, presents an alternative or complementary path to standard therapies.

The present study explored the anti-neoplastic effects of CEP on LUAD cells. As a TCM herb with a broad spectrum of therapeutic applications, CEP has been a staple in cancer treatment for a number of years (25). Isolated from the plant *Stephania cepharantha*, a member of the *Menispermaceae* family, CEP is a marked bisbenzylisoquinoline alkaloid that is uniquely utilized in medical treatments. It has been in medical use in Japan since 1951, primarily to address conditions such as radiation-induced leukopenia and alopecia (43). The existing of research suggests that CEP is safe, with no severe side effects reported. In clinical practice, CEP is frequently applied to counteract leukopenia and leukocyte deficiency resulting from chemotherapy for tumors (44). Previous studies have demonstrated that CEP possesses inhibitory effects on a range of hematological and solid malignancies, including but not limited to leukemia, gastric cancer, ovarian cancer and osteosarcoma. Xu *et al* (45) discovered that CEP effectively modulates numerous signaling pathways, including NF-κB, MAPK and PI3K/Akt/mTOR, in aberrantly activated T cells, exhibits low toxicity and elicits antitumor activity in T cell acute lymphoblastic leukemia. Lu *et al* (46) demonstrated that CEP exerts anti-gastric cancer effects by modulating the nuclear factor erythroid 2-related factor 2/kelch-like ECH-associated protein 1 pathway to induce oxidative stress and modulate energy metabolism. The findings of Su *et al* (35) also underscore the novel anti-neoplastic mechanism of CEP and lend support to its potential as a clinical treatment for hepatocellular carcinoma and other malignancies driven by the Wnt/Hedgehog pathways. In addition, Liang *et al* (24) similarly demonstrated that CEP can suppress the progression of hepatocellular carcinoma (HCC), predominantly by targeting the Janus kinase 2/STAT3 pathway, suggesting that CEP could serve as a viable pharmaceutical option for patients with HCC. Furthermore, Yang *et al* (47) demonstrated that CEP exerts marked pharmacological effects on nasopharyngeal carcinoma, attributed to the inhibition of the EGFR/PI3K/Akt signaling cascade. Notably, a previous study revealed that CEP potently suppresses endogenous anoctamin-1 currents, markedly inhibits the proliferation and migration of LUAD LA795 cells and triggers apoptosis (48). In addition, animal studies have similarly shown that CEP markedly hinders the growth of tumor xenografts in mice (49,50). The present findings indicate that CEP robustly inhibited the proliferation and invasive capacity of two additional LUAD cell lines, H1299

and PC-9, in a dose-dependent manner and further induces apoptosis. These outcomes preliminarily suggest that CEP exerts a suppressive effect on LUAD cells. Notably, the present study also revealed that CEP exerted no discernible toxicity on normal lung epithelial cells. This suggests that CEP could offer a safer alternative to conventional chemotherapy, with a lower risk of side effects, thus holding greater promise as a therapeutic agent for LUAD.

To further explore the mechanisms by which CEP suppresses LUAD progression, the present study incorporated the GSE10799 and GSE31547 datasets, encompassing both LUAD and adjacent non-neoplastic tissue samples and leveraged the STITCH and TCMSP drug target databases to analyze DEGs in LUAD that CEP could potentially regulate. The present bioinformatics analysis identified GPX4 as a probable target gene for CEP in LUAD treatment. GPX dysfunction is associated with a number of cancer types, muscular disorders, cardiovascular conditions, hepatic diseases, renal impairments, neurological diseases and immune system dysfunction (51-54). The selenocysteine residue in GPX is oxidized by hydrogen peroxide (H_2O_2) or other oxidants to form selenic acid, which is then reduced back to selenol through a two-step process involving reactions with GSH. Notably, the selenenic acid intermediate GPX-SeOH can be over-oxidized to seleninic acid under conditions of excessive oxidative stress or depleted GSH levels (55). Among the eight mammalian GPX subtypes, GPX4 contains a selenocysteine residue at its active site and is capable of catalyzing the reduction of H_2O_2 and lipid hydroperoxides with GSH. Uniquely, GPX4 can utilize both GSH and protein thiols as reducing substrates, highlighting its versatility in antioxidant defense (56). The important role of GPX4 in modulating survival is underscored by its mediation of selenium's pro-survival effects in mammals (57). Its activity is pivotal for maintaining cellular homeostasis, curbing reactive oxygen species accumulation and preventing ferroptosis, a form of cell death characterized by its sensitivity to GPX4 inhibition (58). Studies have demonstrated an association between GPX4 expression levels and patient prognosis across a spectrum of cancer types. For example, elevated GPX4 expression in colon adenocarcinoma has been identified as an independent risk factor impacting overall patient survival (59). Similarly, in gastric cancer, increased GPX4 mRNA levels have been associated with adverse patient outcomes, such as worse overall survival (60,61). These findings imply that GPX4 may act as a promoter in the progression of these malignancies. The targeted research on GPX4 has also resulted in the development of novel therapeutics. Protein degraders designed around the heat shock protein 90 molecular chaperone complex aim to trigger cancer cell ferroptosis by degrading endogenous GPX4 (62). In the context of non-small cell lung cancer, where GPX4 expression is markedly upregulated, targeting GPX4 can induce ferroptosis in lung cancer cells, overcoming resistance to EGFR-tyrosine kinase inhibitor therapy (63).

Notably, GPX4 inhibitors such as RAS-selective lethal-3 have been demonstrated to notably suppress the proliferation and migration of lung cancer cells (64). This effect can be reversed by the ferroptosis inhibitor ferrostatin-1, suggesting that GPX4 could represent a new therapeutic target for lung cancer. Beyond its role in ferroptosis, GPX4 also regulates other forms of cell death, including apoptosis, highlighting its multifaceted role in cellular homeostasis. For example, Ding *et al* (65) revealed that GPX4 modulates mitochondrial-mediated apoptosis in triple-negative breast cancer cells through the regulation of early growth response 1. Furthermore, research has indicated that suppressing GPX4 can inhibit plumbagin-induced apoptosis in HCC cells, with the tumor-suppressive effects of plumbagin being associated with the downregulation of GPX4 and the enhancement of apoptotic activity (66). The findings of the present study suggest that the inhibition of GPX4 by CEP may be a key mechanism underlying its anti-tumor effects. In H1299 and PC-9 cells with GPX4 KD, CEP treatment at both concentrations failed to significantly impact cell proliferation, apoptosis or invasive capabilities. This observation indicates that the KD of GPX4 may lead to the loss of CEP therapeutic targets, rendering it ineffective. Similarly, in GPX4 gene-KO mice, the efficacy of CEP was diminished, as evidenced by no significant differences in tumor size, volume and weight between the CEP (5 mg/kg) and CEP (10 mg/kg) treatment groups compared with the PBS control group.

Overall, in the context of the present research, CEP has demonstrated the ability to effectively suppress the proliferation of LUAD cells and growth of xenografted tumors in C57BL/6J mice. However, counteraction of the therapeutic impact of CEP in the event of GPX4 KO suggests that CEP may leverage GPX4 as a molecular target to exert its anti-neoplastic activities. While the present study provides valuable insights into the anti-neoplastic effects of CEP on LUAD cells and its potential as a therapeutic agent, there are still a limitations that warrant acknowledgement. Firstly, although the present bioinformatics analysis identified GPX4 as a potential target gene for CEP in LUAD treatment, the exact molecular mechanisms by which CEP interacts with GPX4 require more detailed investigation. Future studies should aim to elucidate these interactions, potentially through molecular docking studies or other advanced biophysical techniques. Secondly, considering the association between GPX4 and ferroptosis, follow-up studies should aim to further investigate the impact of CEP on ferroptosis in LUAD cells by regulating GPX4. Thirdly, the present study did not extensively explore the potential side effects or toxicity of CEP *in vivo*, which is important in assessing its suitability as a clinical treatment. Long-term studies evaluating the safety profile of CEP in animal models and humans are therefore required. Lastly, the scope of the present study was confined to LUAD and it is unclear whether CEP would exhibit similar effects in other subtypes of lung cancer or other cancer types. Therefore, further research is needed to determine the broader applicability of CEP in cancer treatment. In conclusion, while the present study may lay the groundwork for future investigations into the role of CEP in LUAD and its potential to induce apoptosis, further research is necessary to overcome these limitations and to fully realize the therapeutic potential of CEP.

Acknowledgements

Not applicable.

Funding

The present study was supported by the General Project of Scientific Research Development Fund of Nanjing Medical

University Kangda College (grant no. KD2023KYJJ060) and Lianyungang Cancer Prevention and Treatment Science and Technology Development Program Project (grant no. QN2023010).

Availability of data and materials

The data generated in the present study may be requested from the corresponding author.

Authors' contributions

RC conceptualized the present study, acquired the funding, contributed to the methodology (design and optimization of experimental procedures, establishment of key assays and selection of analytical approaches), provided validation (verification of key findings, confirmation of data consistency across independent experiments and assessment of the reliability of the major experimental results) and wrote, reviewed and edited the manuscript. SK also conceptualized the present study, contributed to the methodology and wrote the original draft. KW collected and organized the raw experimental data, performed quality control checks and performed the experiments. YW curated the data and conducted formal analysis. ML and YZ also conducted formal analysis and project administration. QL was responsible for data management (including data cleaning, normalization and documentation) and performed the statistical analyses. MF acquired the funding, contributed to the the experimental execution, conducted project administration, provided validation and wrote, reviewed and edited the manuscript. RC and MF confirm the authenticity of all the raw data. All authors have read and approved the final version of the manuscript.

Ethics approval and consent to participate

The present animal experiment protocols were approved by the Animal Care and Use Committee of the Second People's Hospital of Lianyungang (approval no. 2023K022) and were performed in accordance with the National Institutes of Health Guide for the Care and Use of Laboratory Animals.

Patient consent for publication

Not applicable.

Competing interests

The authors declare that they have no competing interests.

References

1. Bade BC and Dela Cruz CS: Lung cancer 2020: Epidemiology, etiology, and prevention. Clin Chest Med 41: 1-24, 2020.
2. Nooreldeen R and Bach H: Current and future development in lung cancer diagnosis. Int J Mol Sci 22: 8661, 2021.
3. Li C, Lei S, Ding L, Xu Y, Wu X, Wang H, Zhang Z, Gao T, Zhang Y and Li L: Global burden and trends of lung cancer incidence and mortality. Chin Med J (Engl) 136: 1583-1590, 2023.
4. Petrella F: From diagnosis to treatment of lung cancer: An update in 'cancers' in 2021. Cancers (Basel) 14: 5639, 2022.
5. Wang C, Chen B, Liang S, Shao J, Li J, Yang L, Ren P, Wang Z, Luo W, Zhang L, *et al*: China Protocol for early screening, precise diagnosis, and individualized treatment of lung cancer. Signal Transduct Target Ther 10: 175, 2025.
6. Zhu S, Ge T, Hu J, Jiang G and Zhang P: Prognostic value of surgical intervention in advanced lung adenocarcinoma: A population-based study. J Thorac Dis 13: 5942-5953, 2021.
7. Udelsman BV and Blasberg JD: Advances in surgical techniques for lung cancer. Hematol Oncol Clin North Am 37: 489-497, 2023.
8. Onodera K, Yokota I, Matsumura Y, Hayasaka K, Shiono S, Abe J, Notsuda H, Sakurada A, Suzuki H and Okada Y: Efficacy of platinum-based adjuvant chemotherapy for epidermal growth factor receptor-mutant lung adenocarcinoma. J Thorac Dis 15: 6534-6543, 2023.
9. Cao Y, Lan D, Ke X, Zheng W, Zeng J, Niu N, Fu C, Deng W and Jin S: Investigation of RBM10 mutation and its associations with clinical and molecular characteristics in EGFR-mutant and EGFR-wildtype lung adenocarcinoma. Heliyon 10: e32287, 2024.
10. Canale M, Andrikou K, Priano I, Cravero P, Pasini L, Urbini M, Delmonte A, Crinò L, Bronte G and Ulivi P: The role of TP53 mutations in EGFR-mutated non-small-cell lung cancer: Clinical significance and implications for therapy. Cancers (Basel) 14: 1143, 2022.
11. Zhang J, Wang S, Zhou Z, Lei C, Yu H, Zeng C, Xia X, Qiao G and Shi Q: Unpleasant symptoms of immunotherapy for people with lung cancer: A mixed-method study. Int J Nurs Stud 139: 104430, 2023.
12. Scagliotti GV, Parikh P, von Pawel J, Biesma B, Vansteenkiste J, Manegold C, Serwatowski P, Gatzemeier U, Digumarti R, Zukin M, *et al*: Phase III study comparing cisplatin plus gemcitabine with cisplatin plus pemetrexed in chemotherapy-naive patients with advanced-stage non-small-cell lung cancer. J Clin Oncol 41: 2458-2466, 2023.
13. Matsui Y, Yamada T, Morimoto K, Katayama Y, Hiranuma O, Shiotsu S, Tamiya N, Takeda T, Morimoto Y, Iwasaku M, *et al*: Efficacy and safety of paclitaxel/nab-paclitaxel chemotherapy for patients with relapsed small cell lung cancer. Anticancer Res 42: 4921-4928, 2022.
14. Funaguchi N, Iihara H, Kaito D, Gomyo T, Sasaki Y, Yanase K, Endo J, Ito F, Hirose C, Ohno Y and Okura H: Efficacy of cisplatin plus vinorelbine adjuvant chemotherapy with split-dose administration of cisplatin after complete resection of stage II-IIIA non-small cell lung cancer. Mol Clin Oncol 16: 76, 2022.
15. Zhong J, Zhang Q, Li L and Xu C: Docetaxel plus nedaplatin or carboplatin as second-line chemotherapy for advanced lung squamous cell carcinoma in real-world practice: A single-center experience. Technol Cancer Res Treat 22: 15330338231206334, 2023.
16. Fernandes SS and Saini JK: The impact of chemotherapy on quality of life in advanced-stage lung cancer patients. Indian J Cancer 60: 310-315, 2023.
17. Lv W: Understanding traditional Chinese medicine. Hepatobiliary Surg Nutr 10: 846-848, 2021.
18. Liu Y, Fang C, Luo J, Gong C, Wang L and Zhu S: Traditional Chinese medicine for cancer treatment. Am J Chin Med 52: 583-604, 2024.
19. Wei Z, Chen J, Zuo F, Guo J, Sun X, Liu D and Liu C: Traditional Chinese medicine has great potential as candidate drugs for lung cancer: A review. J Ethnopharmacol 300: 115748, 2023.
20. Xu M, Zhang D and Yan J: Targeting ferroptosis using Chinese herbal compounds to treat respiratory diseases. Phytomedicine 130: 155738, 2024.
21. Miao K, Liu W, Xu J, Qian Z and Zhang Q: Harnessing the power of traditional Chinese medicine monomers and compound prescriptions to boost cancer immunotherapy. Front Immunol 14: 1277243, 2023.
22. Liu Z, Shen S, Wang Y, Sun S, Yu T, Fu Y, Zhou R, Li C, Cao R, Zhang Y, *et al*: The genome of Stephania japonica provides insights into the biosynthesis of cepharanthine. Cell Rep 43: 113832, 2024.
23. Feng Y, He Y, Li Y, Guo W, Gao Y, Zhang J, Kang Y, Lei C, Wang Y and Huang J: Transcriptome analysis of *Stephania cepharantha* and characterization of two CYP80B genes involved in the benzylisoquinoline alkaloid biosynthesis. Plant Physiol Biochem 232: 111088, 2026.
24. Dong X, Zhu W and Wang N: Cepharanthine inhibits the proliferation of glioblastoma cells by blocking the autophagy-lysosomal pathway. Toxicol Appl Pharmacol 493: 117141, 2024.

25. Chen YH, Wu JX, Yang SF, Chen TH, Wu YC, Lin TC and Hsiao YH: Cepharanthine induces oxidative stress and apoptosis in cervical cancer via the Nrf2/Keap1 pathway. Antioxidants (Basel) 14: 1324, 2025.
26. Liang D, Li Q, Du L and Dou G: Pharmacological effects and clinical prospects of cepharanthine. Molecules 27: 8933, 2022.
27. Wang M, Zhang XM, Fu X, Zhang P, Hu WJ, Yang BY and Kuang HX: Alkaloids in genus stephania (*Menispermaceae*): A comprehensive review of its ethnopharmacology, phytochemistry, pharmacology and toxicology. J Ethnopharmacol 293: 115248, 2022.
28. Shi L, Wang S, Zhang S, Wang J, Chen Y, Li Y, Liu Z, Zhao S, Wei B and Zhang L: Research progress on pharmacological effects and mechanisms of cepharanthine and its derivatives. Naunyn Schmiedebergs Arch Pharmacol 396: 2843-2860, 2023.
29. Sun F, Liu J, Tariq A, Wang Z, Wu Y and Li L: Unraveling the mechanism of action of cepharanthine for the treatment of novel coronavirus pneumonia (COVID-19) from the perspectives of systematic pharmacology. Arab J Chem 16: 104722, 2023.
30. Xia B, Zheng L, Li Y, Sun W, Liu Y, Li L, Pang J, Chen J, Li J and Cheng H: The brief overview, antivirus and anti-SARS-CoV-2 activity, quantitative methods, and pharmacokinetics of cepharanthine: A potential small-molecule drug against COVID-19. Front Pharmacol 14: 1098972, 2023.
31. Iqbal A, Najam R, Simjee S, Athar Ishaqui A, Ashfaq Ahmad S, Ahmed Z, Ahmed S, Ahmed S, Jaweed L, Maboos M, *et al*: Cepharanthine action in preventing obesity and hyperlipidemia in rats on a high-fat high sucrose diet. Saudi Pharm J 30: 1683-1690, 2022.
32. Chen G, Wen D, Shen L, Feng Y, Xiong Q, Li P and Zhao Z: Cepharanthine exerts antioxidant and anti-inflammatory effects in lipopolysaccharide (LPS)-induced macrophages and DSS-induced colitis mice. Molecules 28: 6070, 2023.
33. Wang Y, Wang T, Wang H, Liu W, Li X, Wang X and Zhang Y: A mechanistic updated overview on Cepharanthine as potential anticancer agent. Biomed Pharmacother 165: 115107, 2023.
34. Liang Y, Li J, Xu H, Pang M, Hu C, Weng X and Xie W: Cepharanthine suppresses proliferation and metastasis and enhances apoptosis by regulating JAK2/Stat3 pathway in hepatocellular carcinoma. Cell Mol Biol (Noisy-le-grand) 69: 94-100, 2023.
35. Su GF, Huang ZX, Huang DL, Chen PX, Wang Y and Wang YF: Cepharanthine hydrochloride inhibits the Wnt/β-catenin/Hedgehog signaling axis in liver cancer. Oncol Rep 47: 83, 2022.
36. Livak KJ and Schmittgen TD: Analysis of relative gene expression data using real-time quantitative PCR and the 2(-Delta Delta C(T)) method. Methods 25: 402-408, 2001.
37. Wang Y, Zhou Z, Chen L, Li Y, Zhou Z and Chu X: Identification of key genes and biological pathways in lung adenocarcinoma via bioinformatics analysis. Mol Cell Biochem 476: 931-939, 2021.
38. Dai JJ, Zhou WB and Wang B: Identification of crucial genes associated with lung adenocarcinoma by bioinformatic analysis. Medicine (Baltimore) 99: e23052, 2020.
39. Ritchie ME, Phipson B, Wu D, Hu Y, Law CW, Shi W and Smyth GK: limma powers differential expression analyses for RNA-sequencing and microarray studies. Nucleic Acids Res 43: e47, 2015.
40. Bayne K: Revised guide for the care and use of laboratory animals available. American physiological society. Physiologist 39: 199, 208-211, 1996.
41. Seguin L, Durandy M and Feral CC: Lung adenocarcinoma tumor origin: A guide for personalized medicine. Cancers (Basel) 14: 1759, 2022.
42. Lahiri A, Maji A, Potdar PD, Singh N, Parikh P, Bisht B, Mukherjee A and Paul MK: Lung cancer immunotherapy: Progress, pitfalls, and promises. Mol Cancer 22: 40, 2023.
43. Liu K, Hong B, Wang S, Lou F, You Y, Hu R, Shafqat A, Fan H and Tong Y: Pharmacological activity of cepharanthine. Molecules 28: 5019, 2023.
44. Kamei S, Tanaka R, Hirakawa H, Iwao M, Kawanaka R, Tatsuta R, Terao T and Itoh H: A case of improvement of clozapine-induced low leukocyte counts by adenine, cepharanthin and ninjin-yoei-to in a patient with treatment-resistant schizophrenia. J Pharm Health Care Sci 7: 45, 2021.
45. Xu W, Chen S, Wang X, Tanaka S, Onda K, Sugiyama K, Yamada H and Hirano T: Molecular mechanisms and therapeutic implications of tetrandrine and cepharanthine in T cell acute lymphoblastic leukemia and autoimmune diseases. Pharmacol Ther 217: 107659, 2021.
46. Lu YY, Zhu CY, Ding YX, Wang B, Zhao SF, Lv J, Chen SM, Wang SS, Wang Y, Wang R, *et al*: Cepharanthine, a regulator of keap1-Nrf2, inhibits gastric cancer growth through oxidative stress and energy metabolism pathway. Cell Death Discov 9: 450, 2023.
47. Yang J, Qin L, Zhou S, Li J, Tu Y, Mo M, Liu X, Huang J, Qin X, Jiao A, *et al*: Network pharmacology, molecular docking and experimental study of CEP in nasopharyngeal carcinoma. J Ethnopharmacol 323: 117667, 2024.
48. Tang ZH, Cao WX, Guo X, Dai XY, Lu JH, Chen X, Zhu H and Lu JJ: Identification of a novel autophagic inhibitor cepharanthine to enhance the anti-cancer property of dacomitinib in non-small cell lung cancer. Cancer Lett 412: 1-9, 2018.
49. Zhang X, Zhang G, Zhao Z, Xiu R, Jia J, Chen P, Liu Y, Wang Y and Yi J: Cepharanthine, a novel selective ANO1 inhibitor with potential for lung adenocarcinoma therapy. Biochim Biophys Acta Mol Cell Res 1868: 119132, 2021.
50. Seubwai W, Vaeteewoottacharn K, Hiyoshi M, Suzu S, Puapairoj A, Wongkham C, Okada S and Wongkham S: Cepharanthine exerts antitumor activity on cholangiocarcinoma by inhibiting NF-kappaB. Cancer Sci 101: 1590-1595, 2010.
51. Handy DE and Loscalzo J: The role of glutathione peroxidase-1 in health and disease. Free Radic Biol Med 188: 146-161, 2022.
52. Brigelius-Flohé R and Flohé L: Regulatory phenomena in the glutathione peroxidase superfamily. Antioxid Redox Signal 33: 498-516, 2020.
53. Yang WS, SriRamaratnam R, Welsch ME, Shimada K, Skouta R, Viswanathan VS, Cheah JH, Clemons PA, Shamji AF, Clish CB, *et al*: Regulation of ferroptotic cancer cell death by GPX4. Cell 156: 317-331, 2014.
54. Zhang W, Liu Y, Liao Y, Zhu C and Zou Z: GPX4, ferroptosis, and diseases. Biomed Pharmacother 174: 116512, 2024.
55. Ursini F and Maiorino M: Lipid peroxidation and ferroptosis: The role of GSH and GPx4. Free Radic Biol Med 152: 175-185, 2020.
56. Li FJ, Long HZ, Zhou ZW, Luo HY, Xu SG and Gao LC: System X_c^-/GSH/GPX4 axis: An important antioxidant system for the ferroptosis in drug-resistant solid tumor therapy. Front Pharmacol 13: 910292, 2022.
57. Alim I, Caulfield JT, Chen Y, Swarup V, Geschwind DH, Ivanova E, Seravalli J, Ai Y, Sansing LH, Marie EJS, *et al*: Selenium drives a transcriptional adaptive program to block ferroptosis and treat stroke. Cell 177: 1262-1279.e25, 2019.
58. Ma T, Du J, Zhang Y, Wang Y, Wang B and Zhang T: GPX4-independent ferroptosis-a new strategy in disease's therapy. Cell Death Discov 8: 434, 2022.
59. Pavliuk-Karachevtseva A, Mihalik J, Biel R, Rybárová S and Hodorová I: Chosen antioxidant enzymes GPx4 and GPx8 in human colorectal carcinoma: Study of the Slovak population. Medicina (Kaunas) 58: 298, 2022.
60. Sugezawa K, Morimoto M, Yamamoto M, Matsumi Y, Nakayama Y, Hara K, Uejima C, Kihara K, Matsunaga T, Tokuyasu N, *et al*: GPX4 regulates tumor cell proliferation via suppressing ferroptosis and exhibits prognostic significance in gastric cancer. Anticancer Res 42: 5719-5729, 2022.
61. Lee J and Roh JL: Targeting GPX4 in human cancer: Implications of ferroptosis induction for tackling cancer resilience. Cancer Lett 559: 216119, 2023.
62. Liu B and Qian D: Hsp90α and cell death in cancers: A review. Discov Oncol 15: 151, 2024.
63. Ahn MJ, Sun JM, Lee SH, Ahn JS and Park K: EGFR TKI combination with immunotherapy in non-small cell lung cancer. Expert Opin Drug Saf 16: 465-469, 2017.
64. Zheng C, Wang C, Sun D, Wang H, Li B, Liu G, Liu Z, Zhang L and Xu P: Structure-activity relationship study of RSL3-based GPX4 degraders and its potential noncovalent optimization. Eur J Med Chem 255: 115393, 2023.
65. Ding Y, Chen X, Liu C, Ge W, Wang Q, Hao X, Wang M, Chen Y and Zhang Q: Identification of a small molecule as inducer of ferroptosis and apoptosis through ubiquitination of GPX4 in triple negative breast cancer cells. J Hematol Oncol 14: 19, 2021.
66. Yao L, Yan D, Jiang B, Xue Q, Chen X, Huang Q, Qi L, Tang D, Chen X and Liu J: Plumbagin is a novel GPX4 protein degrader that induces apoptosis in hepatocellular carcinoma cells. Free Radic Biol Med 203: 1-10, 2023.